

H.J. Völk · E.G. Berezhko · L.T. Ksenofontov

# New evidence for strong nonthermal effects in Tycho's supernova remnant

Received: date / Accepted: date

**Abstract** For the case of Tycho's supernova remnant (SNR) we present the relation between the blast wave and contact discontinuity radii calculated within the nonlinear kinetic theory of cosmic ray (CR) acceleration in SNRs. It is demonstrated that these radii are confirmed by recently published Chandra measurements which show that the observed contact discontinuity radius is so close to the shock radius that it can only be explained by efficient CR acceleration which in turn makes the medium more compressible. Together with the recently determined new value  $E_{\text{sn}} = 1.2 \times 10^{51}$  erg of the SN explosion energy this also confirms our previous conclusion that a TeV  $\gamma$ -ray flux of  $(2-5) \times 10^{-13}$  erg/(cm<sup>2</sup>s) is to be expected from Tycho's SNR. Chandra measurements and the HEGRA upper limit of the TeV  $\gamma$ -ray flux together limit the source distance  $d$  to  $3.3 \leq d \leq 4$  kpc.

**Keywords** (ISM:)cosmic rays – acceleration of particles – shock waves – supernovae individual(Tycho's SNR) – radiation mechanisms:non-thermal – gamma-rays:theory

## 1 Introduction

Cosmic rays (CRs) are widely accepted to be produced in SNRs by the diffusive shock acceleration process at the outer blast wave (see e.g. [17, 13, 6, 21, 23] for reviews). Kinetic nonlinear theory of diffusive CR acceleration in SNRs [7, 8] couples the gas dynamics of the explosion with the particle acceleration. Therefore in a spherically symmetric approach it is able to predict the evolution of gas density, pressure, mass velocity, as well as the positions of the forward shock and the contact discontinuity, together with the energy spectrum and the spatial distribution of CR nuclei and electrons at any given evolutionary epoch  $t$ , including the properties of the nonthermal radiation. The application of this theory

to individual SNRs [9, 10, 11, 28] has demonstrated its power in explaining the observed SNR properties and in predicting new effects like the extent of magnetic field amplification, leading to the concentration of the highest-energy electrons in a very thin shell just behind the shock.

Recent observations with the *Chandra* and *XMM-Newton* X-ray telescopes in space have confirmed earlier detections of nonthermal continuum emission in hard X-rays from young shell-type SNRs. With *Chandra* it became even possible to resolve spatial scales down to the arcsec extension of individual dynamical structures like shocks [27, 22, 3]. The filamentary hard X-ray structures are the result of strong synchrotron losses of the emitting multi-TeV electrons in amplified magnetic fields downstream of the outer accelerating SNR shock [27, 10, 12, 30]. Such observational results gain their qualitative significance through the fact that these effective magnetic fields and morphologies turned out to be exactly the same as predicted theoretically from acceleration theory.

This theory has been applied in detail to Tycho's SNR, in order to compare results with the existing data [28, 30]. We have used a stellar ejecta mass  $M_{ej} = 1.4M_{\odot}$ , distance  $d = 2.3$  kpc, and interstellar medium (ISM) number density  $N_H = 0.5$  H-atoms cm<sup>-3</sup>. For these parameters a total hydrodynamic explosion energy  $E_{\text{sn}} = 0.27 \times 10^{51}$  erg was derived to fit the observed size  $R_s$  and expansion speed  $V_s$ . A rather high downstream magnetic field strength  $B_d \approx 300 \mu\text{G}$  and a proton injection rate  $\eta = 3 \times 10^{-4}$  are needed to reproduce the observed steep and concave radio spectrum and to ensure a smooth cutoff of the synchrotron emission in the X-ray region. We believe that the required strength of the magnetic field, that is significantly higher than the MHD compression of a  $5 \mu\text{G}$  ISM field, has to be attributed to nonlinear field amplification at the SN shock by CR acceleration itself. According to plasma physical considerations [24, 5, 4], the existing ISM magnetic field can indeed be significantly amplified at a strong shock by CR streaming instabilities.

After adjustment of the predictions of the nonlinear spherically-symmetric model by a physically necessary renormalization of the number of accelerated CR nuclei to take account of the quasi-perpendicular shock directions in a SNR,

H.J. Völk  
Max Planck Institut für Kernphysik, Postfach 103980, D-69029 Heidelberg, Germany E-mail: Heinrich.Voelk@mpi-hd.mpg.de

E.G. Berezhko · L.T. Ksenofontov  
Yu.G. Shafer Institute of Cosmophysical Research and Aeronomy, 31 Lenin Ave., 677980 Yakutsk, Russia

very good consistency with the existing observational data was achieved.

Using *Chandra* X-ray observations [32] have recently estimated the ratio between the radius  $R_c$  of the contact discontinuity (CD), separating the swept-up ISM and the ejecta material, and the radius  $R_s$  of the forward shock. The large mean value  $R_c/R_s = 0.93$  of this ratio was interpreted as evidence for efficient CR acceleration, which makes the medium between those two discontinuities more compressible.

Here we present the calculations of the mean ratio  $R_c/R_s$ , which are the unchanged part of our earlier considerations [28,30], and demonstrate that these results, which are in fact predictions, fit the above measurements very well. Since our calculations have been made in spherical symmetry they concern a priori an azimuthally averaged ratio  $R_c/R_s$ . We shall extend them by taking the effects of the Rayleigh-Taylor (R-T) instability of the CD into account. We shall in addition discuss a physical mechanism that leads to the observed *azimuthal* variations of  $R_c/R_s$ . Finally we shall take the recent determination of the mechanical energy output  $E_{\text{sn}} \approx 1.2 \times 10^{51}$  [2] which results from the theory of delayed detonations in the physics of type Ia SN explosions [19,20], in order to predict a range for the  $\gamma$ -ray spectrum that is consistent with the existing upper limits of high energy  $\gamma$ -ray fluxes from Tycho's SNR.

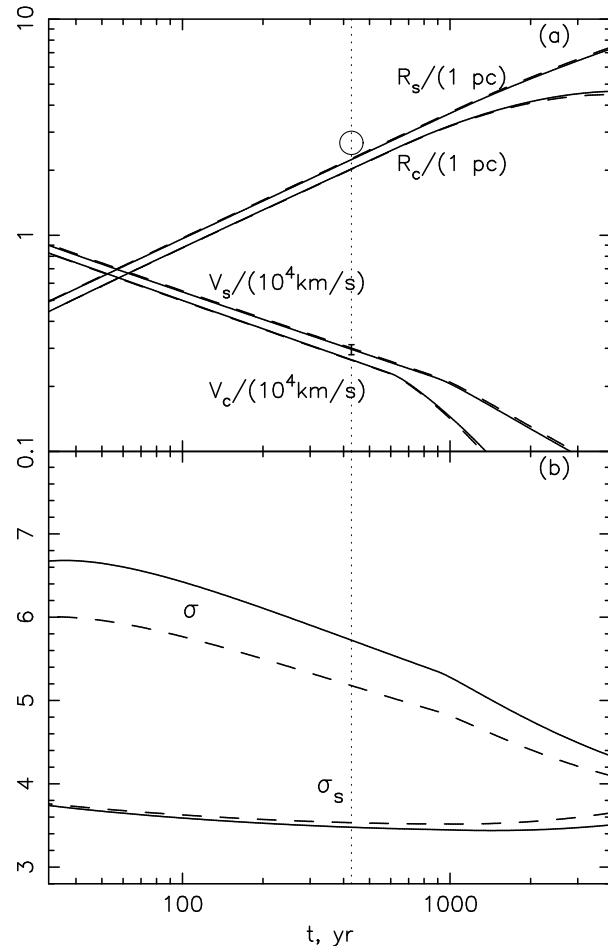
## 2 Results and Discussion

Fig.1 and partly Fig.2 show the calculations of shock and CD related quantities which were part of our earlier considerations [28,30]. The calculated shock as well as CD radii and speeds are shown as a function of time for the two different cases of interior magnetic field strengths  $B_d = 240 \mu\text{G}$  and  $B_d = 360 \mu\text{G}$  considered, together with the azimuthally averaged experimental data available at the time.

According to Fig.1a Tycho is nearing the adiabatic phase. To fit the spectral shape of the observed radio emission we assumed a proton injection rate  $\eta = 3 \times 10^{-4}$ . This leads to a significant nonlinear modification of the shock at the current age of  $t = 428$  yrs. A larger magnetic field lowers the Alfvénic Mach number and therefore leads to a decrease of the shock compression ratio, as seen in Fig.1b. The result is a total compression ratio  $\sigma = 5.7$  and a subshock compression ratio  $\sigma_s = 3.5$  for  $B_d = 240 \mu\text{G}$ . In turn  $\sigma = 5.2$ ,  $\sigma_s = 3.6$ , for  $B_d = 360 \mu\text{G}$ .

Therefore, as can be seen from Fig.2, including CR acceleration at the outer blast wave, the calculated value of the ratio  $R_c/R_s$  for  $B_d = 360 \mu\text{G}$  is slightly lower than for  $B_d = 240 \mu\text{G}$ . At the current epoch we have  $R_c/R_s \approx 0.90$  which is lower than the value  $R_c/R_s = 0.93$  inferred from the observations. Qualitatively our result goes in the same direction as calculations by [14] which modeled SNRs with a uniform specific heat ratio  $\gamma_{\text{eff}} < 5/3$ , for the circumstellar medium and the ejecta material alike.

Projecting a highly structured shell onto the plane of the sky tends to favor protruding parts of the shell. Therefore the



**Fig. 1** (a) Shock radius  $R_s$ , contact discontinuity radius  $R_c$ , shock speed  $V_s$ , and contact discontinuity speed  $V_c$ , for Tycho's SNR as functions of time, including particle acceleration; (b) total shock ( $\sigma$ ) and subshock ( $\sigma_s$ ) compression ratios. The dotted vertical line marks the current epoch. The solid and dashed lines correspond to the internal magnetic field strength  $B_d = 240 \mu\text{G}$  and ( $B_d = 360 \mu\text{G}$ ), respectively. The observed mean size and speed of the shock, as determined by radio measurements [26], are shown as well.

average radius measured in projection is an overestimate of the true average radius. Analysing the amount of bias from the projection for the shock and CD radii [32] found a corrected "true" value  $R_c/R_s = 0.93$  which is lower than their measured "projected average" value  $R_c/R_s = 0.96$ , as a result of the above geometrical effect.

In turn, starting from a spherically symmetric calculation of the CD radius, as we do, one has to take into account that the actual CD is subject to the R-T instability. In the nonlinear regime it leads to effective mixing of the ejecta and swept-up ISM material with "fingers" of the ejecta on top of this mixing region, which extend farther into the shocked gas than the radius  $R_c$  predicted when assuming spherical symmetry e.g. [16, 18, 14, 31]. Therefore our ratio  $R_c/R_s = 0.90$ , calculated within the spherically symmetric approach, has to be corrected for this effect in order to compare it with the measured value  $R_c/R_s = 0.93$ . In the case when all the fin-

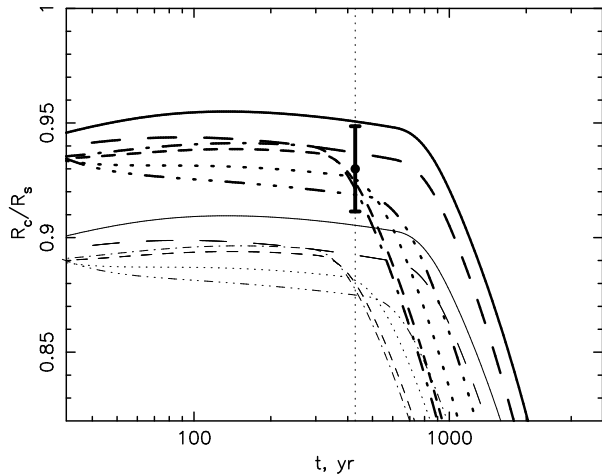


**Fig. 2** The ratio  $R_c/R_s$  of the radii of the contact discontinuity and the forward shock as a function of time. *Solid and dashed* lines correspond to the same two cases as in Fig.1. The lines of all other styles correspond to the SN explosion energy  $E_{\text{sn}} = 1.2 \times 10^{51}$  erg and four different distances (see the caption of Fig.3) *Thin* lines represent the values calculated in the spherically symmetric model, whereas the *thick* lines show the values  $R'_c/R_s$  which contain the correction for the effect produced by the R-T instability. The experimental point is taken from [32].

gers have length  $l$  and occupy half of the CD surface, one would have a mean CD size  $R'_c \approx R_c + 0.5l$  which has to be compared with  $0.93R_s$ . According to the numerical modelling of [31], albeit without particle acceleration, the R-T instability allows fingers of ejecta to protrude beyond the spherically symmetric CD radius by 10%. The longest fingers of size  $l \approx 0.1R_c$  occupy less than 50% of the CD surface. However, in projection they stick out of the mixing region, whose thickness is roughly  $0.5l$ . This leads to a rough estimate of the corrected CD radius  $R'_c = 1.05R_c$  which has to be compared with the experimentally estimated value.

The comparison of the corrected values  $R'_c/R_s$ , according to our earlier calculations as well as for different assumptions (see below) about the explosion energy and source distance, with this experimentally estimated value  $R_c/R_s = 0.93$  (in Fig.2 we present that value with 2% uncertainties, according to [32]) shows quite good agreement (see Figs.2 and 3) even if one takes into account some uncertainty in the quantitative determination of our correction factor  $R'_c/R_c$ , which in our view lies in the range 1.03-1.07.

Another interesting peculiarity of Tycho's shock structure, which we would like to discuss here, is the quite irregular behaviour of the radius of the forward shock around the edge of the visible SNR disk, that is clearly seen in Fig.3. Large shock distortions of this kind are not expected to result from the R-T instability. At first sight such a variation of the values of  $R_s$  and  $R_c$  can be easily attributed to fluctuations of the ambient ISM density and/or to an inhomogeneously distributed density and velocity field of the ejected matter. The local shock part, which encounters a lower ISM density or has a faster ejecta portion behind, propagates faster compared with the neighbouring shock pieces. This will lead to

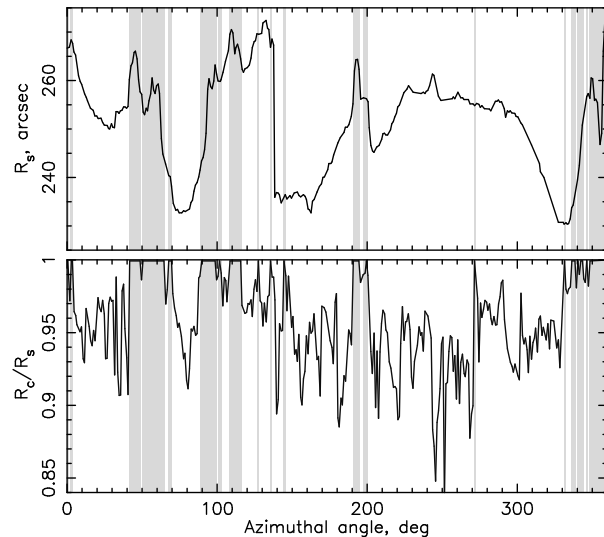


**Fig. 3** *Top panel:* the forward shock radius  $R_s$  and *bottom panel:* the ratio  $R_c/R_s$  of the radii of the contact discontinuity and the forward shock as a function of azimuthal angle [32]. The regions where  $R_c/R_s > 0.99$  are shadowed.

the formation of local forward displacements of the CD and the forward shock whose number and relative sizes are determined by the specific structure of the ISM and/or ejecta. Since a larger shock compression ratio is expected for higher shock speed (see Fig.1b), one should also expect a smaller difference between  $R_s$  and  $R_c$  on the top region of each such displacement. This is exactly what is observed.

Such arguments would give a good explanation for the observed picture only if CR injection/acceleration took place uniformly across the entire shock surface. However, in our view the actual situation is expected to be more complicated – and physically more interesting. Efficient injection of suprathermal nuclear particles into the acceleration process takes place in those local shock regions, where the forward shock is quasi-parallel, and these regions are distributed over the shock surface according to the ambient ISM magnetic field structure and occupy in total about 20% of the shock [29]. As a result one would expect that only about 20% of the local forward shock displacements efficiently accelerate nuclear CRs, and therefore display the extraordinary high ratio  $R_c/R_s$ . In reality the most extreme values  $R_c/R_s \geq 0.99$  are observed on randomly distributed local shock regions, and the positions of these regions roughly coincide with the positions of extended shock displacements. To explain such a correlation a strong physical connection between the shock speed and the efficiency of CR injection/acceleration should exist: the local parts of the shock with large speed effectively produce CRs and vice versa.

There are at least two physical processes which can resolve the above problem. The first one gives high injection on the leading part of the displacements, if they are formed due to ISM and/or ejecta inhomogeneities and initially the injection was suppressed here as a result of a highly oblique magnetic field. Since after its formation the leading part of

the displacement develops a large curvature, it will have a significant portion which becomes quasi-parallel, and therefore efficient CR injection/acceleration is expected over the whole leading part of such a displacement.

The second factor can presumably itself lead to the formation of displacements, even in the case of a uniform ISM and a spherically symmetric ejecta distribution. A significant fraction of the internal energy behind a quasi-parallel part of the shock front is contained in CRs. Since the shock is expected to be modified, the CR spectrum is very hard and therefore the pressure is mainly carried by the CRs with the highest energies. With their high mobility these CRs can diffuse laterally into neighbouring downstream volumes, which are located behind shock surfaces not producing CRs. This diffusive loss leads to a decrease of the internal pressure behind the quasi-parallel parts of the shock. Therefore the corresponding downstream ejecta undergo less deceleration. As a result these ejecta accelerate relative to their surroundings. This leads to the formation of a local displacement. One can expect that this also distorts the initially spherically symmetric shock. We therefore conclude that the effectively accelerating parts of the forward shock are among those regions, where the displacements occur, and they may actually delineate them. Predominantly fingers are situated on the effectively accelerating parts of the shock surface. If this is correct it gives a unique experimental identification of the areas at the outer SNR shock which efficiently produce nuclear CRs.

Since the most outwardly displaced parts of the CD and the shock with a high ratio  $R_c/R_s$  have to be interpreted as the regions with efficient CR injection/acceleration, this opens the possibility to experimentally distinguish the shock areas with efficient CR production from those where CRs are not produced. A rough estimate shows that in Tycho's SNR the regions with extremely high ratios  $R_c/R_s > 0.99$  and the displacements occupy about 20% of the shock surface see Fig.4 of [32]. This corresponds to the theoretical expectation.

Our last point regards constraints which the recent re-evaluation of the mechanical output  $E_{\text{sn}} = 1.2 \times 10^{51}$  erg together with the *HEGRA* upper limit for the TeV  $\gamma$ -ray flux [1] approximately impose on the distance and ambient density for Tycho's SNR. With this new  $E_{\text{sn}}$ -value we find a consistent fit for all existing data – the SNR size, its expansion rate, overall synchrotron spectrum and the filament structure of the X-ray emission – like it was done for the previously defined explosion energy  $E_{\text{sn}} = 0.27 \times 10^{51}$  erg (see [28,30] for details). In particular, the fit of  $R_s$  and  $V_s$ , which is of the same quality as in Fig.1 for  $E_{\text{sn}} = 0.27 \times 10^{51}$  erg, gives for each assumed distance  $d$  a rather definite value of the ISM number density  $N_{\text{H}}(d)$ . A rough explanation of this numerical result is the following: since for a given experimentally measured angular SNR size and its expansion rate the linear size  $R_s$  and the speed  $V_s$  scale proportionally to distance  $d$ , and since in the nearby (in time) Sedov phase  $R_s \propto (E_{\text{sn}}/N_{\text{H}})^{1/5}$ , the density  $N_{\text{H}} \propto E_{\text{sn}}/d^5$  decreases with increasing distance  $d$ . The hadronic  $\gamma$ -ray flux

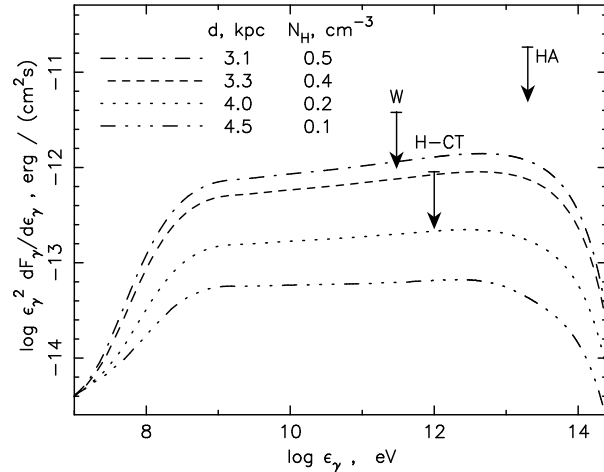


**Fig. 4** Spectral energy distribution of the  $\gamma$ -ray emission from Tycho's SNR, as a function of  $\gamma$ -ray energy  $\epsilon_\gamma$ , for a mechanical SN explosion energy of  $E_{\text{sn}} = 1.2 \times 10^{51}$  erg and four different distances  $d$  and corresponding values of the ISM number densities  $N_{\text{H}}$ . All cases have a dominant hadronic compared to Inverse Compton  $\gamma$ -ray flux. Experimental data are the upper limits of the *HEGRA* (H-CT; [1]) and *Whipple* (W; [15]) Cherenkov telescopes and the 95% confidence *HEGRA AIROBICC* (HA; [25]) upper limit.

$F_\gamma \propto R_s^3 V_s^2 N_{\text{H}}^2 / d^2$  is then expected to scale as  $F_\gamma \propto E_{\text{sn}}^2 / d^7$ . The ejected mass is still assumed to be  $M_{\text{ej}} = 1.4 M_\odot$ . We also find the same nuclear injection rate  $\eta = 3 \times 10^{-4}$  for all cases, and downstream magnetic field values  $B_d \approx 400 \mu\text{G}$ . At the same time, the linear size  $L$  of an X-ray filament increases proportional to  $d$ . Therefore the magnetic field strength  $B'_d \propto L^{-2/3}$  [12], determined from the filament sizes (see Introduction), decreases with  $d$ .

In order to find the constraint on the distance  $d$  and the ISM density  $N_{\text{H}}$ , we then compare in Fig.3 the resulting  $\gamma$ -ray spectral energy distribution with the *HEGRA* and *Whipple* upper limits at TeV energies. It is seen that all distances  $d < 3.3$  kpc are inconsistent with the *HEGRA* data. Distances of  $d > 4$  kpc are still consistent with the  $\gamma$ -ray data, although there is a growing discrepancy between  $B_d$  and  $B'_d$ : at  $d = 4.5$  kpc  $B'_d \approx 300 \mu\text{G}$  which is already considerably smaller than  $B_d \approx 400 \mu\text{G}$ . Therefore we believe that we can constrain the source distance also from above,  $d < 4$  kpc. In Fig.2 we also show the values for  $R_c/R_s$  and  $R'_c/R_s$  for the case  $E_{\text{sn}} = 1.2 \times 10^{51}$  erg and these increased distances. Within our approximate determination of  $R'_c$  from  $R_c$  they still agree with the *Chandra* data, in particular because the CR production rates are comparable. Our calculations of the  $\gamma$ -ray emission lead us to predict that the new Northern Hemisphere TeV detectors should detect this source at TeV-energies in, predominantly, hadronic  $\gamma$ -rays: the expected  $\pi^0$ -decay  $\gamma$ -ray energy flux  $(2-5) \times 10^{-13}$  erg/(cm<sup>2</sup>s) extends up to almost 100 TeV if the distance is indeed within the range 3.3-4 kpc. As a corollary the detection of a TeV signal is not only important by itself, but it is also crucial for the correct determination of all other key Supernova parameters.

**Acknowledgements** EGB and LTK acknowledge the partial support by the Presidium of RAS (program No.16) and by the SB RAS (CIP-2006 No.3.10) and the hospitality of the Max-Planck-Institut für Kernphysik, where part of this work was carried out.

## References

1. Aharonian, F.A., Akhperjanian, A., Barrio, J. et al.: A study of Tycho's SNR at TeV energies with the HEGRA CT-System. *A&A* **373**, 292–300 (2001)
2. Badenes, C., Borkowski, K.J., Hughes, J.P., et al.: Constraints on the Physics of Type Ia Supernovae from the X-Ray Spectrum of the Tycho Supernova Remnant. *ApJ* **645**, 1373–1391 (2006)
3. Bamba, A., Yamazaki, R., Ueno, M., Koyama, K.: Small-Scale Structure of the SN 1006 Shock with Chandra Observations. *ApJ* **589**, 827–837 (2003)
4. Bell, A.R.: Turbulent amplification of magnetic field and diffusive shock acceleration of cosmic rays. *MNRAS* **353**, 550–558 (2004)
5. Bell, A. R., Lucek, S.G.: Cosmic ray acceleration to very high energy through the non-linear amplification by cosmic rays of the seed magnetic field. *MNRAS* **321**, 433–438 (2001)
6. Berezhko, E.G., Krymsky, G.F.: Acceleration of cosmic rays by shock waves. *Soviet Phys.-Uspekhi* **12**, 155 (1988)
7. Berezhko, E.G., Elshin, V.K., Ksenofontov, L.T.: Cosmic Ray Acceleration in Supernova Remnants. *JETP* **82**, 1–21 (1996)
8. Berezhko, E.G., Völk, H.J.: Kinetic theory of cosmic rays and gamma rays in supernova remnants. I. Uniform interstellar medium. *Astropart. Phys.* **7**, 183–202 (1997)
9. Berezhko, E.G., Ksenofontov, L.T., Völk, H.J.: Emission of SN 1006 produced by accelerated cosmic rays. *A&A* **395**, 943–953 (2002)
10. Berezhko, E.G., Ksenofontov, L.T., Völk, H.J.: Confirmation of strong magnetic field amplification and nuclear cosmic ray acceleration in SN 1006. *A&A* **412**, L11–L14 (2003)
11. Berezhko, E. G.; Pühlhofer, G.; Völk, H. J.: Gamma-ray emission from Cassiopeia A produced by accelerated cosmic rays. *A&A* **400**, 971–980 (2003)
12. Berezhko, E.G., Völk, H.J.: Direct evidence of efficient cosmic ray acceleration and magnetic field amplification in Cassiopeia A. *A&A* **419**, L27–L30 (2004)
13. Blandford, R.D., Eichler, D.: Particle Acceleration at Astrophysical Shocks — a Theory of Cosmic-Ray Origin. *Phys. Rept.* **154**, 1 (1987)
14. Blondin, J.M., Ellison, D.C.: Rayleigh-Taylor Instabilities in Young Supernova Remnants Undergoing Efficient Particle Acceleration. *ApJ* **560**, 244–253 (2001)
15. Buckley, J.H., Akerlof, C.W., Carter-Lewis, D.A., et al.: Constraints on cosmic-ray origin from TeV gamma-ray observations of supernova remnants. *A&A* **329**, 639–658 (1998)
16. Chevalier, R.A., Blondin, J.M., Emmering, R.T.: Hydrodynamic instabilities in supernova remnants — Self-similar driven waves. *ApJ* **392**, 118–130 (1992)
17. Drury, L'O.C.: An introduction to the theory of diffusive shock acceleration of energetic particles in tenuous plasmas. *Rep. Progr. Phys.* **46**, 973–1027 (1983)
18. Dwarkadas, V.V.: Interaction of Type IA Supernovae with Their Surroundings: The Exponential Profile in Two Dimensions. *ApJ* **541**, 418–427 (2000)
19. Gamezo, V.N., Khokhlov, A.M., Oran, E.S.: Deflagrations and Detonations in Thermonuclear Supernovae. *Phys. Rev. Lett.* **92**, 211102 (2004)
20. Gamezo, V.N., Khokhlov, A.M., Oran, E.S.: Three-dimensional Delayed-Detonation Model of Type Ia Supernovae. *ApJ* **623**, 337–346 (2005)
21. Jones, F.C., Ellison, D.C.: The plasma physics of shock acceleration. *Space Sci. Rev.* **58**, 259–346 (1991)
22. Long, K.S., Reynolds, S.P., Raymond, J.C., et al.: Chandra CCD Imagery of the Northeast and Northwest Limbs of SN 1006. *ApJ* **586**, 1162–1178 (2003)
23. Malkov, M.A., Drury, L.O'C.: Nonlinear theory of diffusive acceleration of particles by shock waves. *Rep. Prog. Phys.* **64**, 429–481 (2001)
24. Lucek, S.G., Bell, A.R.: Non-linear amplification of a magnetic field driven by cosmic ray streaming. *MNRAS* **314**, 65–74 (2000)
25. Prah, J., Prosch, C.: in Proc. 25th ICRC (Durban) **3**, 217–220 (1997)
26. Tan, S.M., Gull, S.F.: The expansion of Tycho's supernova remnant as determined by a new algorithm for comparing data. *MNRAS* **216**, 949–970 (1985)
27. Vink, J., Laming, J.M.: On the Magnetic Fields and Particle Acceleration in Cassiopeia A. *ApJ* **584**, 758–769 (2003)
28. Völk, H.J., Berezhko, E.G., Ksenofontov, L.T., Rowell, G.P.: The high energy gamma-ray emission expected from Tycho's supernova remnant. *A&A* **396**, 649–656 (2002)
29. Völk, H.J., Berezhko, E.G., Ksenofontov, L.T.: Variation of cosmic ray injection across supernova shocks. *A&A* **409**, 563–571 (2003)
30. Völk, H.J., Berezhko, E.G., Ksenofontov, L.T.: Magnetic Field Amplification in Tycho and other Shell-type Supernova Remnants. *A&A* **433**, 229–240 (2005)
31. Wang, C.-Y., Chevalier, R.A.: Instabilities and Clumping in Type IA Supernova Remnants. *ApJ* **549**, 1119–1134 (2001)
32. Warren, J.S., Hughes, J.P., Badenes, C. et al.: Cosmic-Ray Acceleration at the Forward Shock in Tycho's Supernova Remnant: Evidence from Chandra X-Ray Observations. *ApJ* **634**, 376–389 (2005)